JAAS

Cite this: *J. Anal. At. Spectrom.*, 2011, **26**, 2247

www.rsc.org/jaas

PAPER

Effect of damping force on CIT and QIT ion traps supplied with a periodic impulse voltage form

S. M. Sadat Kiai,[a] S. Seddighi Chaharborj,*[b] M. R. Abu Bakar[b] and I. Fudziah[b]

Received 3rd June 2011, Accepted 26th July 2011
DOI: 10.1039/c1ja10170f

The behavior of confined ions under a damping force based on laser or collisional cooling is of particular importance in different disciplines especially in high resolution mass spectrometry. The significance of the effect of the damping force on confined ions in a cylindrical ion trap has not been yet investigated, so, in this article a cylindrical ion trap excited with a periodic impulse voltage of the form $f(t) = V_0 cos\Omega t/(1 - kcos2\Omega t)$ with $0 \leq k < 1$ is studied and compared to the quadrupole ion trap with and without the effect of damping force. Numerical computations allowed the determination of the twelve stability diagrams using fifth order Runge–Kutta derivative approximations. The physical properties of the confined ions in the r and z axis are illustrated and the effect of damping force on the fractional mass resolutions $m/\Delta m$ of the confined ions in two first and second stability regions of both ion traps was analyzed.

1. Introduction

Ion trap mass spectrometry has developed through several stages to their current stage of relatively high performance and increasing popularity.[17,18] Quadrupole ion trap (QIT) invented by Paul and Steinwedel[21] has been widely applied to mass spectrometry,[17,18,25–28] ion cooling and spectroscopy,[10,11,34] frequency standards,[22,33] quantum computing,[12,31] and so on. To apply to various objectives, various geometries of ion trap for the mass spectrometer have been suggested.[3]

A QIT is a combination of electric or magnetic fields that captures ions in a region of a vacuum system or tube. The QIT have a number of scientific uses such as trapping ions while the ion's quantum state is manipulated, and mass spectrometry. When using ion traps for scientific studies of quantum state manipulation, the Paul trap is most often used. This work may lead to a trapped ion quantum computer[4] and has already been used to create the worlds most accurate atomic clocks.[24]

An ion trap mass spectrometer may incorporate a Penning trap,[5] Paul trap[7] or the Kingdon trap.[13] The Orbitrap, introduced in 2005, is based on the Kingdon trap.[9] The two most common types of ion traps are the Penning trap and the Paul trap (quadrupole ion trap). Other types of mass spectrometers may also use a linear quadrupole ion trap as a selective mass filter. Computation of stability regions is of particular importance in order to design and assemble an ion trap. Analytical and matrix methods, on one hand, have been widely used to calculate the stability regions.[1,2,14]

A quadrupole ion trap mass analyzer with simplified geometry, the cylindrical ion trap (CIT), was shown to be well-suited to use in miniature mass spectrometers and even mass spectrometer arrays. Experiments with a single miniature CIT showed acceptable resolution and sensitivity, limited by the ion trapping capacity of the miniature device.[23]

In a cylindrical ion trap, the hyperbolic ring electrode is replaced by a simple cylinder and the two hyperbolic end cap electrodes are replaced by two planar endplate electrodes (See Fig. (1)).

The (CIT) has received much attention from a number of research groups because of several merits. The CIT is easier to fabricate than the Paul ion trap which has hyperbolic surfaces,[19] and the relative simplicity and small size of the CIT make it an ideal candidate for miniaturization. With these interests, many groups in Purdue University[36] and Oak Ridge National Laboratory,[15,16] for example, have researched the applications of the CIT to a miniaturized mass spectrometer.

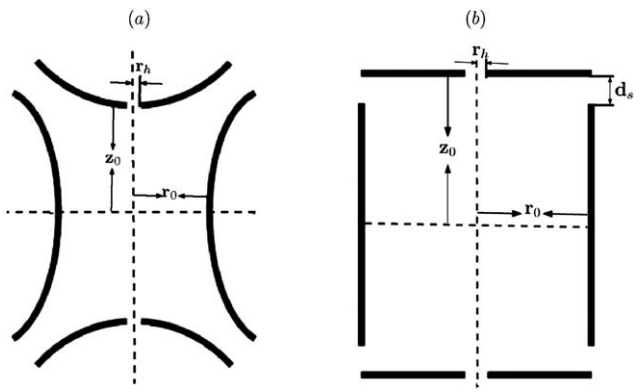

Fig. 1 Cross section of (a) Paul Trap, (b) Cylindrical Ion Trap (CIT). Here d_s is the spacing between ring and end-cap electrodes.

[a]*Nuclear Science Research School and Technology Research Institute (NSTRI), P. O. Box 14395-836, Tehran, Iran*
[b]*Department of Mathematics, Faculty of Science, Universiti Putra Malaysia, 43400 UPM, Malaysia. E-mail: sarkhosh@math.upm.edu.my; Fax: +60389437958; Tel: +60389437958*

In our previous paper,[30] we have studied the properties of ions confined in a CIT supplied with a periodic impulse voltage of the form $V_{ac}cost/(1 - kcos(2t))$ with $0 \leq k < 1$ and compared to the Paul ion trap. In this article, the effect of damping force on an ion movement and the fractional mass resolution in a CIT and QIT supplied with a periodic impulse voltage form is studied and compared.

1.1. Damping force

In physics and engineering, damping may be mathematically modelled as a force synchronous with the velocity of the object but opposite in direction to it. If such force is also proportional to the velocity, as for a simple mechanical viscous damper, the force F may be related to the velocity v by

$$F = -cv,$$

where c is the viscous damping coefficient, given in units of Newton-seconds per meter.[32,35,37] This force is an approximation to the friction caused by drag.[8] Here $c = lm$, where the parameter m denotes the mass of the ion and l is a constant. In physics, damping is any effect that tends to reduce the amplitude of oscillations in an oscillatory system, particularly the harmonic oscillator. There are two kinds of damping forces; the first kind is due to the collisions of ion with the photons of the laser used for cooling purposes, and another one is related to the collisions of ions with the photons of the laser used for cooling purposes. For collisions with gas molecules, the constant l is extracted by the mobility data for specified ions and buffer gases into the trap, and depends on the pressure and temperature of the gas as follows,[6]

$$l = \frac{q}{M}\frac{1}{\mu}.$$

The reduced mobility μ_0 is also given by the following expression,[6]

$$\mu_0 = \mu\frac{273.16K}{T}\frac{p}{1013\ \text{mbar}}.$$

Here T and p are the temperature of the buffer gas in K and its pressure in mbar, respectively.

1.2. Ion movement in CIT

Fig. (1) show the electronics configuration of CIT, that is to say a combinations of d.c. voltage, U_{dc}, and an alternative voltage $V_{ac}f(t)$ with $f(t) = V_0 cos\Omega t/(1 - kcos2\Omega t)$ with $0 \leq k < 1$ is the modulation "index" parameter for the ring and end-caps electrodes,

$$\Psi_0 = \pm(U_{dc} - V_{ac}\cos\Omega t/(1 - kcos2\Omega t)) \quad \text{with} \quad 0 \leq k < 1 \quad (1)$$

then the potential distribution inside the CIT at any point of a circle of radius r can be written as:

$$\Psi(r, z) = \sum_i \frac{2\Psi_0}{m_i r_1}\frac{J_0(m_i r)}{J_1(m_i r_1)}\frac{ch(m_i z)}{ch(m_i z_1)}. \quad (2)$$

Here J_0 and J_1 are the Bessel functions of first kind, of order 0 and order 1, respectively, ch is the hyperbolic *cosine* function, $m_i r$ is roots of equation $J_0(m_i r) = 0$, U_{dc} and V_{ac} are the amplitudes and the radio frequency (rf) drive frequency. Assuming that $r_1^2 = 2z_1^2$, then the electric field in a cylindrical coordinates (r, z, θ) inside the CIT can be written:

$$(E_r, E_\theta, E_z) = E = -\nabla\Psi(r, z). \quad (3)$$

Here ∇ is gradient and from eqn (3) we have,

$$\begin{aligned} E_r &= \sum_i \frac{2\Psi_0}{r_1}.\frac{J_1(m_i r)}{J_1(m_i r_1)}.\frac{ch(m_i z)}{ch(m_i z_1)}, \\ E_\theta &= 0, \\ E_z &= -\sum_i \frac{2\Psi_0}{r_1}.\frac{J_0(m_i r)}{J_1(m_i r_1)}.\frac{sh(m_i z)}{ch(m_i z_1)}, \end{aligned} \quad (4)$$

The basic equation of the ion motions of mass m and electric charge e into the trap taking into account the effect of damping force may be treated independently:

$$\begin{aligned} &\frac{d^2u}{d\tau^2} + 2K'\frac{du}{d\tau} - (\alpha - 2\chi\cos 2\tau/(1 - kcos4\tau)). \\ &\sum_i \frac{J_1(\lambda_i u)}{J_1(\lambda_i)}.\frac{ch(\lambda_i v)}{ch\left(\lambda_i\frac{z_1}{r_1}\right)} = 0, \\ &\frac{d^2v}{d\tau^2} + 2K'\frac{du}{d\tau} + (\alpha - 2\chi\cos 2\tau/(1 - kcos4\tau)). \\ &\sum_i \frac{J_0(\lambda_i u)}{J_1(\lambda_i)}.\frac{sh(\lambda_i v)}{ch\left(\lambda_i\frac{z_1}{r_1}\right)} = 0, \end{aligned} \quad (5)$$

with the following substitutions:

$$\tau = \frac{\Omega t}{2}, \quad m_i r_1 = \lambda_i, \quad \frac{r}{r_1} = u, \quad \frac{z}{r_1} = v,$$

$$\alpha = -8\frac{e}{m}\times\frac{U_{dc}}{r_1^2\Omega^2}, \ \chi = 4\frac{e}{m}\times\frac{(1-k)V_{ac}}{r_1^2\Omega^2}, \ K' = \frac{c}{m\Omega}, \quad (6)$$

where α and χ are the trapping parameters, $\lambda_i = m_i r_1$ is roots of equation $J_0(m_i r_1) = 0$, $c = lm$ (l is constant) and K' is damping factor.

Let us assume a hyperbolic geometry for the Paul ion trap supplied with a periodic impulse voltage form,

$$\left(\frac{z}{z_0}\right)^2 - \left(\frac{r}{r_0}\right)^2 = \pm 1, \quad \text{and} \quad r_0^2 = 2z_0^2. \quad (7)$$

The ion motions of an ion of mass m and charge e with the effect of damping force in each of the perpendicular directions r and z, may be treated independently as follows,

$$\frac{d^2u}{d\tau^2} + 2K''\frac{du}{d\tau} + (a - 2q\cos 2\tau/(1 - kcos\,4\tau))u = 0, \quad (8)$$

in which u is one of the directions r and z, and with the following substitutions:

$$\begin{aligned} &\tau = \frac{\Omega t}{2}; \quad u = r \text{ or } z, \\ &a_z = -2a_r = -4\frac{e}{m}\times\frac{U}{z_0^2\Omega^2}, \\ &q_z = -2q_r = 2\frac{e}{m}\times\frac{(1-k)V}{z_0^2\Omega^2}, \ K'' = \frac{c'}{m\Omega}, \end{aligned} \quad (9)$$

where $c' = l'm$ (l' is constant), $\Omega/2\pi$ is the radio frequency (rf) drive frequency, z_0 is one-half the shortest separation of the end cap electrodes, $r_0^2 = 2z_0^2$ is the square of ring electrode radius, a_z and q_z are the trapping parameters and K'' is the damping force.

1.3. Expression of trapping parameters

If we consider ions of the same species and if it applies to both type of cages of potential difference of same amplitude and same frequency, then we have the following relationship between the parameters α and χ on one side and a_z and q_z on the other:

$$\frac{\alpha}{a_z} = 2\frac{z_0^2}{r_1^2} \quad \text{and} \quad \frac{\chi}{q_z} = 2\frac{z_0^2}{r_1^2}. \tag{10}$$

From eqn (10) and $r_0^2 = 2z_0^2$ we have

$$\alpha = a_z\left(\frac{r_0}{r_1}\right)^2 \quad \text{and} \quad \chi = q_z\left(\frac{r_0}{r_1}\right)^2. \tag{11}$$

Eqn (11) with effect of damping force can be expressed as follows,

$$\alpha = a_z\left(\frac{K'}{K''}\right)^2\left(\frac{c'}{c}\right)^2\left(\frac{r_0}{r_1}\right)^2 \quad \text{and} \quad \chi = q_z\left(\frac{K'}{K''}\right)^2\left(\frac{c'}{c}\right)^2\left(\frac{r_0}{r_1}\right)^2. \tag{12}$$

Here K', the damping force and $c = lm$ (l is constant) are the damping parameters for CIT and K'', the damping force and $c' = l'm$ (l' is constant) are the damping parameters for QIT.

Notation. The value of the damping parameters K' and K'' determine the behavior of the CIT and QIT systems as follows,

- K', $K'' > 1$ is overdamped: The system returns to equilibrium without oscillating. Larger values of the damping parameters K', $K'' > 1$ return to equilibrium slower.
- K', $K'' = 1$ is critically damped: The system returns to equilibrium as quickly as possible without oscillating. This is often desired for the damping of systems such as doors.
- K', $K'' < 1$ is underdamped: The system oscillates with the amplitude gradually decreasing to zero.

In this paper we use K', $K'' = 0$ for without damping force and K', $K'' = 1$ for with damping force.

2. Results

2.1. Stability regions without damping force and $k = 0$

To compute the accurate elements of the motion equations for the stability diagrams, a fifth order Runge–Kutta method is employed. Fig. (2a and b) presents the calculated stability regions

$$A_0 = -\frac{1}{2}q^2 + \frac{7}{128}q^4 - \frac{29}{2304}q^6 + \frac{68687}{18874368}q^8 - \frac{123707}{104857600}q^{10} + \ldots,$$

$$A_1 = \frac{1}{4}q^2 - \frac{7}{1024}q^4 + \frac{29}{73728}q^6 - \frac{68687}{2415919104}q^8 + \frac{123707}{53687091200}q^{10} + \ldots,$$

$$\vdots$$

$$B_1 = 1 - q - \frac{1}{8}q^2 + \frac{1}{64}q^3 - \frac{1}{1536}q^4 - \frac{11}{36864}q^5 + \frac{49}{589824}q^6 + \ldots,$$

$$B_2 = -2 + q + \frac{1}{16}q^2 - \frac{1}{256}q^3 + \frac{1}{12288}q^4 + \frac{11}{589824}q^5 - \frac{49}{18874368}q^6 + \ldots,$$

$$\vdots$$

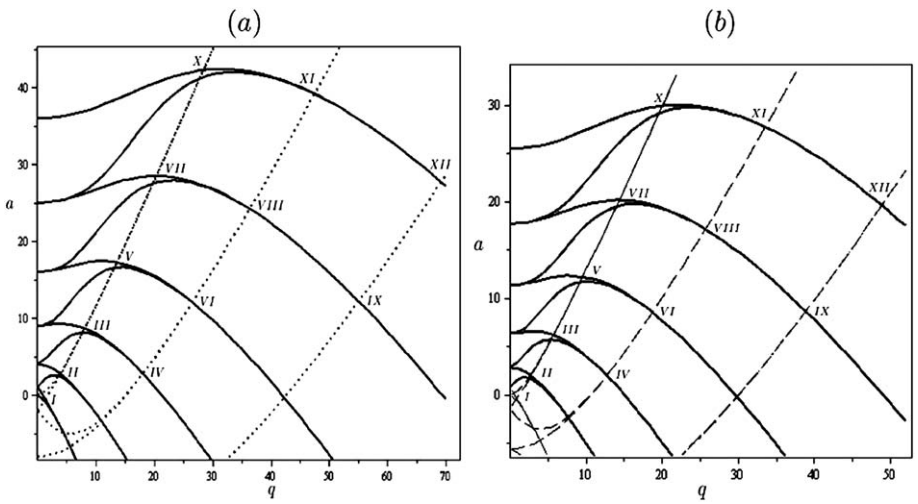

Fig. 2 (*a*) The stability regions *I* until *XII* for the CIT, (*b*) The stability regions *I* until *XII* for the QIT without damping force and $k = 0$.

I until XII for CIT and QIT, respectively, using 0.0001 steps increment in fifth order Runge–Kutta method. Table (1) and Table (2) show the values of (a, q) and ($\alpha/2$, $\chi/2$) at the lower and upper tips of the twelve stability regions of a QIT and CIT computed in this article for $k = 0$, respectively. To find the values of (a, q) we have used the equations A_0, A_1,… and B_1, B_2,…, to get the intersection point as follows,

The computed twelfth stability diagrams presented here, Fig. (2), is just to show how they behave as we go from lower to higher stability regions. Of course in practice, it's the first region which has the largest area for the ion confinement. However, what can be concluded from these results is that, we can see a similar demonstration between classical QIT and CIT for the different regions; a reduction in stability regions as the regions number increases.

2.2. Stability regions with damping force and without damping force

Fig. (3a and b) show the first and the second stability regions for QIT and CIT with damping force and without damping force when $k = 0$ and $k = 0.9$, respectively. And the parameters are defined as follows; A_1 and A_2 are the first and the second stability regions for QIT when $K'' = 1$. A_1 and A_2 are the first and the second stability regions for QIT when $K'' = 0$, B_1 and B_2 are the first and the second stability regions for CIT when $K' = 1$ and

Table 1 The values of a and q at the lower and upper tips of the twelve stability regions of a QIT computed in this article for $k = 0$

	a		q	
Region no.	Lower tip	Upper tip	Lower tip	Upper tip
I	−0.6713	0.1499	0.0000	1.3512
II	2.4106	2.8431	3.5210	3.9822
III	8.1284	8.6431	7.7103	8.1120
IV	2.7812	2.8142	18.0341	18.0712
V	16.5203	17.2650	13.1201	13.5810
VI	12.0470	12.0592	26.5309	26.5431
VII	27.5601	28.4352	18.8102	20.3620
VIII	24.2085	24.2205	36.3579	36.3675
IX	12.1840	12.1845	55.0513	55.0520
X	41.1810	42.2703	27.7750	28.4152
XI	39.1738	39.1859	47.5151	47.5254
XII	27.6914	27.6916	69.1921	69.1923

Table 2 The values of $\alpha/2$ and $\chi/2$ at the lower and upper tips of the twelve stability regions of a CIT computed in this article for $k = 0$

	$\alpha/2$		$\chi/2$	
Region no.	Lower tip	Upper tip	Lower tip	Upper tip
I	−0.4747	0.1061	0.0000	0.9555
II	1.7046	2.0082	2.4890	2.8158
III	5.7476	6.1377	5.4518	5.7346
IV	1.9666	1.9898	12.7520	12.7783
V	11.6814	12.2082	9.2772	9.6025
VI	8.5185	8.5271	18.7602	18.7687
VII	19.4879	20.1066	13.5623	14.3967
VIII	17.1182	17.1265	25.7089	25.7157
IX	8.6154	8.6158	38.9271	38.9276
X	29.1186	29.8894	19.6399	20.0924
XI	27.7001	27.7086	33.5983	33.6055
XII	19.5808	19.5809	48.9262	48.9263

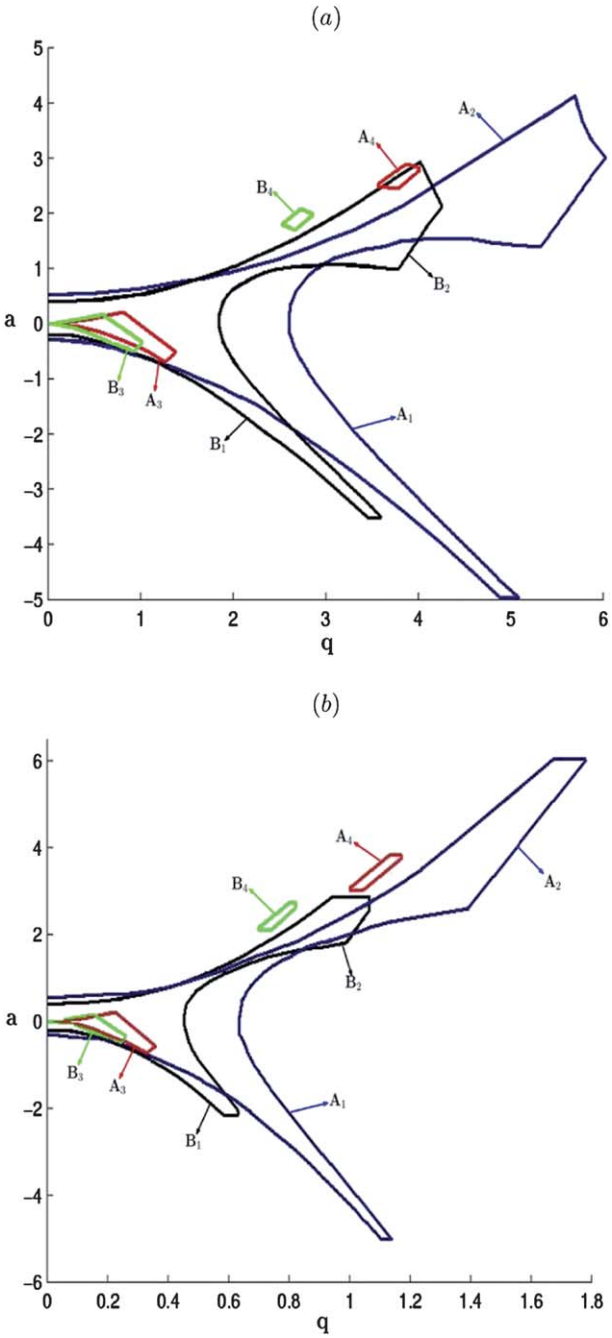

Fig. 3 (a) The first and second stability regions for QIT and CIT with damping force and without damping force when $k = 0$. (b) The first and second stability regions for QIT and CIT with damping force and without damping force when $k = 0.9$. Here, A_1: The first stability region for QIT when $K'' = 1$, A_2: The second stability region for QIT when $K'' = 1$, A_3: The first stability region for QIT when $K'' = 0$, A_4: The second stability region for QIT when $K'' = 0$, B_1: The first stability region for CIT when $K' = 1$, B_2: The second stability region for CIT when $K' = 1$, B_3: The first stability region for CIT when $K' = 0$, B_4: The second stability region for CIT when $K' = 0$.

finally, B_3 and B_4 are the first and the second stability regions for CIT when $K' = 0$.

What one can extract from the results obtained for the Stability regions with and without damping force is the general expansion form which is almost the same except for the sizes. In general, a reduction in an a and q stability diagram will demand more confining voltage for the same ion mass-to-charge ratio and for the enlargement is vice verse.

As will be seen later, this expansion of the stability diagram in the a and q region due to the damping force will affect the mass resolution of the devices in a way that more confining voltage will be presented between the ions mass-to-charge ratios. For example, if the trap function in an rf only mode, there will be more V_{ac} voltage needed to reach the mass instability conditions, compared to the case of without damping force.

2.3. Ion trajectories

Table (3) shows the values of q and χ of QIT and CIT, respectively with damping force and without damping force for the equivalent points; two operating points located in their corresponding stability diagram having the same $\beta_z : \beta_z = 0.3; 0.6; 0.95$ and $k = 0; 0.9$. For the computations, the following formulas have been used,

$$\frac{a-\beta^2}{q} = \frac{1}{\frac{a-\beta^2}{q} - \frac{1}{\frac{a-(2+\beta)^2}{q} - \frac{1}{\frac{a-(4+\beta)^2}{q} - \ldots}}} + \frac{1}{\frac{a-\beta^2}{q} - \frac{1}{\frac{a-(\beta-2)^2}{q} - \frac{1}{\frac{a-(\beta-4)^2}{q} - \ldots}}}, \tag{13}$$

$$\frac{a-\beta^2+2K''\beta}{q} = \frac{1}{\frac{a-\beta^2+2K''\beta}{q} - \frac{1}{\frac{a-(2+\beta)^2+2K''(2+\beta)}{q} - \frac{1}{\frac{a-(4+\beta)^2+2K''(4+\beta)}{q} - \ldots}}} + \frac{1}{\frac{a-\beta^2+2K''\beta}{q} - \frac{1}{\frac{a-(\beta-2)^2+2K''(\beta-2)}{q} - \frac{1}{\frac{a-(\beta-4)^2+2K''(\beta-4)}{q} - \ldots}}}. \tag{14}$$

Here eqn (13) is without damping force and eqn (14) is with damping force.

2.4. Fractional resolution

The resolution of a quadrupole ion trap[29] and cylindrical ion trap mass spectrometry in general, is a function of the mechanical accuracy of the hyperboloid of the QIT Δr_0, and the cylindrical of the CIT Δr_1, and the stability performances of the electronics device such as, variations in voltage amplitude ΔV, the rf frequency $\Delta\Omega$[20] and Δk ($0 \leq k < 1$), which tell us how accurate the form of the voltage signal is. The factor Δk plays an important role in building the stability diagrams for the purpose of the mass resolution. $\Delta k = 0$ is an ideal case for higher resolution value.

Table 3 The values of q and χ for QIT and CIT with "QITDF", "CITDF" and without damping force, respectively, for $\beta_z = 0.3; 0.6; 0.95$ and $k = 0; 0.9$

		q		χ	
β_z	k	QIT	QITDF	CIT	CITDF
0.3	0.0	0.4094	1.1048	0.8189	2.1837
0.3	0.9	0.0409	0.1105	0.0819	0.2184
0.6	0.0	0.7324	1.9764	1.4648	3.9063
0.6	0.9	0.0732	0.1976	0.1465	0.3906
0.95	0.0	0.9052	2.4426	1.8104	4.8278
0.95	0.9	0.0905	0.2443	0.1810	0.4828

To derive a useful theoretical formula for the fractional resolution, one has to recall the stability parameters of the impulse excitation for the QIT and CIT

$$q_z = 4\frac{e}{m} \times \frac{V_k(1-k)}{r_0^2\Omega^2}, \tag{15}$$

$$\chi = 4\frac{e}{m} \times \frac{(V_{ac})_k(1-k)}{r_1^2\Omega^2} \tag{16}$$

By taking the partial derivatives with respect to the variables of the stability parameters q_z for eqn (15) and χ for eqn (16), then the expression of the resolution Δm of the QIT and CIT are as follows,

$$\Delta m = \left(\frac{8eV_k(1-k)}{r_0^3\Omega^2 q_z}\right)|\Delta r_0| + \left(\frac{4e(1-k)}{r_0^2\Omega^2 q_z}\right)|\Delta V| + \left(\frac{8eV_k(1-k)}{r_0^2\Omega^3 q_z}\right)|\Delta\Omega| + \left(\frac{4eV_k}{r_0^2\Omega^2 q_z}\right)|\Delta k|, \tag{17}$$

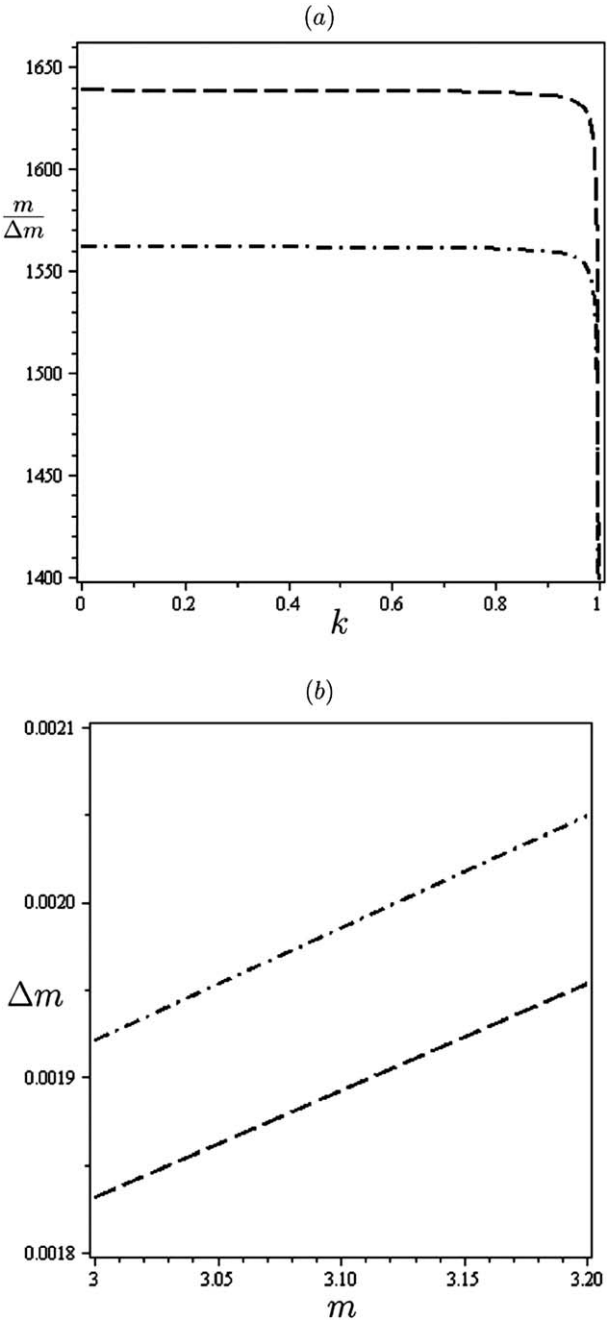

Fig. 4 (a) The fractional resolution as a function of the modulation "index" parameter k, dash line is without damping force, dash dot line is with damping force, (b) resolution of Δm as function of ion mass m, dash line is without damping force and dash dot line is with damping force.

$$\Delta m = \left(\frac{8e(V_{ac})_k(1-k)}{r_1^3\Omega^2\chi}\right)|\Delta r_1| + \left(\frac{4e(1-k)}{r_0^2\Omega^2\chi}\right)|\Delta V_{ac}| + \left(\frac{8e(V_{ac})_k(1-k)}{r_1^2\Omega^3\chi}\right)|\Delta\Omega| + \left(\frac{4e(V_{ac})_k}{r_1^2\Omega^2\chi}\right)|\Delta k|. \quad (18)$$

Now to find the fractional resolution we have,

$$\frac{m}{\Delta m} = \left\{\left|\frac{\Delta V}{V}\right| + 2\left|\frac{\Delta\Omega}{\Omega}\right| + 2\left|\frac{\Delta r_0}{r_0}\right| + \left|\frac{\Delta k}{1-k}\right|\right\}^{-1}, \quad (19)$$

$$\frac{m}{\Delta m} = \left\{\left|\frac{\Delta V_{ac}}{V_{ac}}\right| + 2\left|\frac{\Delta\Omega}{\Omega}\right| + 2\left|\frac{\Delta r_1}{r_1}\right| + \left|\frac{\Delta k}{1-k}\right|\right\}^{-1}, \quad (20)$$

here eqn (19) and eqn (20) are the fractional resolutions for QIT and CIT, respectively. We have used the stability parameters a_z and q_z to establish the first stability diagrams in the (U, V_{ac}) plane. The following parameters are used: $r_0 = 10$ mm, $\Omega = 2\pi f = 2\pi \times 650 \times 10^3$ rad s^{-1}, $k = 0$ and 0.9 and for the mass range of $m = 1$, 2, and 3 a.m.u. (hydrogen and hydrogen like isotopes). Fig. (4a and b), presents the effect

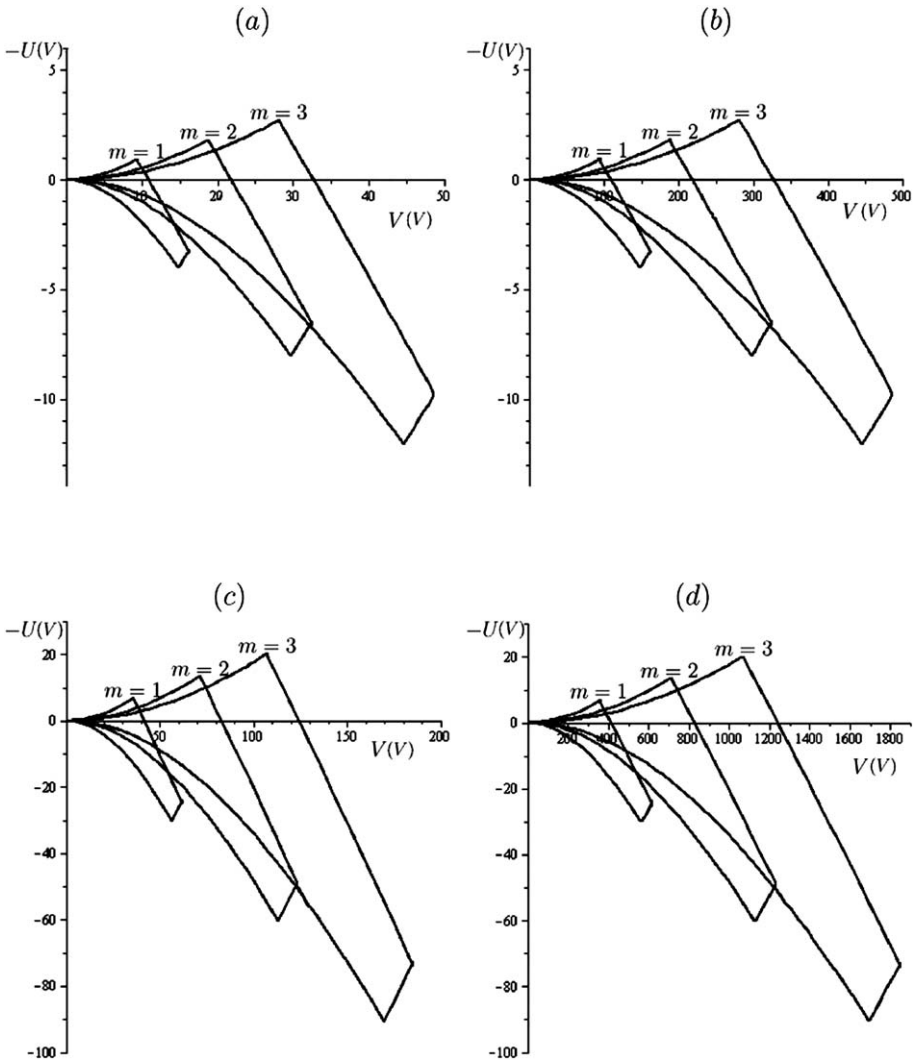

Fig. 5 (a) and (b) the stability diagram in (U, V) plan in the QIT without damping force for $m = 1,2,3$ and (a) $k = 0$, (b) $k = 0.9$. (c) and (d) the stability diagram in (U, V) plan in the QIT with damping force for $m = 1$, 2, 3 and (c) $k = 0$, (d) $k = 0.9$.

of damping force on the fractional resolutions as a function of k and m. As seen in Fig. (4), damping force affects considerably the fractional resolution. The computed stability diagrams in (U, V_{ac}) plane for QIT and CIT with and without damping force are depicted in Fig. (5) and Fig. (6) and their lower and upper limits are displayed in Table (4) and Table (5). From Fig. (5) and Fig. (6), it can be seen that, the size of stability diagrams for the same masses are much larger for the $k = 0.9$ than the sinusoidal classical mode $k = 0$ in both QIT and CIT especially when damping force is applied. This means that, more confining voltage needed for $k = 0.9$ than $k = 0$ for the same ion mass-to-charge ration.

As for $m = 3$ a.m.u., $k = 0.9$ and $U = 0$, the limited confining voltage for QIT with and without damping force are about 1232.713 (V) and 326.571 (V), respectively, as for CIT are 1755.204 (V) and 461.241 (V). One can see that, the limits of confining voltage ratio for damping are the same in QIT and CIT. The same ratio also can be found for QIT and CIT when $k = 0$. As far as the fractional resolution is concerned, we have considered only eqn (17) for the cases of $k = 0$ and $k = 0.9$, as it will be the same treatment for eqn (18). For the fractional mass resolution we have used the following uncertainties for the voltage, rf frequency and the geometry; $\Delta v/v = 10^{-5}$, $\Delta\Omega/\Omega = 10^{-7}$, $\Delta r_0/r_0 = 3 \times 10^{-4}$ for $k = 0$ and for $k = 0.9$ we have taken arbitrary the modulation "index" parameter $\Delta k = 10^{-7}$. The fractional resolutions obtained are $m/\Delta m = 1638.8$ for $k = 0$ and $m/\Delta m = 1636.1$ for $k = 0.9$ for the case of without damping force. When damping is applied, the rf only limited voltage is increased by the factor of approximately 4, therefore, we have taken the voltage uncertainties as $\Delta v/v = 4 \times 10^{-5}$ and $m/\Delta m = 1559.5$. When these fractional resolutions are considered for the tritium isotope mass $m = 3.02348$, then, we have $\Delta m = 0.001938$ and 0.001847 for the damping and without damping force. This means that, as the value of $m/\Delta m$ is decreased, the power of resolution is increased due to increment in Δm. Experimentally, this means that the width of the mass signal spectra is better separated. Table (6) shows the limited confining voltage for QIT and CIT with and without damping force for $m = 1$, 2, 3 a.m.u., $k = 0$, 0.9 and $U = 0$.

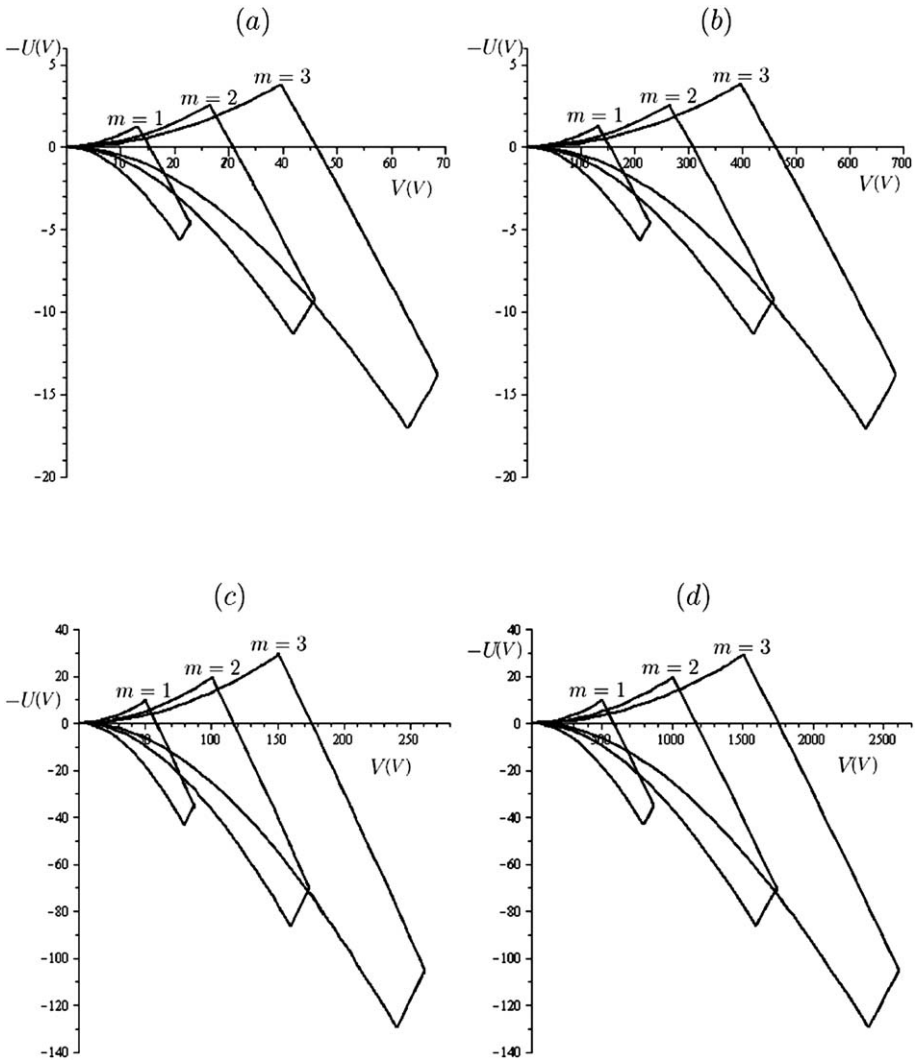

Fig. 6 (a) and (b) the stability diagram in (U, V) plan in the CIT without damping force for $m = 1, 2, 3$ and (a) $k = 0$, (b) $k = 0.9$. (c) and (d) the stability diagram in (U, V) plan in the CIT with damping force for $m = 1, 2, 3$ and (c) $k = 0$, (d) $k = 0.9$.

Table 4 The values of ($-U$, V) at the lower and upper tips of the first stability regions of a QIT computed in this article for $m = 1, 2, 3$ and $k = 0, 0.9$. Here "LT" is Lower tip and "UT" is Upper tip

		QIT				QITDF			
		$-U$		V		$-U$		V	
m	k	LT	UT	LT	UT	LT	UT	LT	UT
1	0.0	−4.053	0.913	0.000	16.183	−29.971	6.492	0.000	61.273
1	0.9	−4.053	0.913	0.000	161.83	−29.971	6.492	0.000	612.734
2	0.0	−8.074	1.772	0.000	32.346	−59.960	13.315	0.000	122.673
2	0.9	−8.074	1.772	0.000	323.46	−59.960	13.315	0.000	1226.732
3	0.0	−12.091	2.714	0.000	48.371	−90.292	19.442	0.000	184.382
3	0.9	−12.091	2.714	0.000	483.710	−90.292	19.442	0.000	1843.801

Table 5 The values of $(-U, V)$ at the lower and upper tips of the first stability regions of a CIT computed in this article for $m = 1, 2, 3$ and $k = 0, 0.9$. Here "LT" is Lower tip and "UT" is Upper tip

		CIT				CITDF			
		$-U$		V_{ac}		$-U$		V_{ac}	
m	k	LT	UT	LT	UT	LT	UT	LT	UT
1	0.0	−5.642	1.213	0.000	22.751	−42.673	9.253	0.000	87.072
1	0.9	−5.642	2.213	0.000	227.510	−42.673	9.253	0.000	870.724
2	0.0	−11.315	2.456	0.000	45.908	−86.414	11.867	0.000	173.572
2	0.9	−11.315	2.456	0.000	459.081	−86.414	11.867	0.000	1735.723
3	0.0	−17.024	3.753	0.000	68.461	−129.196	28.471	0.000	260.226
3	0.9	−17.024	3.753	0.000	684.613	−129.196	28.471	0.000	2602.263

Table 6 The limited confining voltage for QIT and CIT with and without damping force for $m = 1, 2, 3$ a.m.u., $k = 0, 0.9$ and $U = 0$

		V		V_{ac}	
m	k	QIT	QITDF	CIT	CITDF
1	0.0	10.593	41.093	15.274	58.437
1	0.9	105.932	410.934	152.742	584.375
2	0.0	21.625	81.582	30.882	116.634
2	0.9	216.257	815.826	308.823	1166.341
3	0.0	32.657	123.271	46.124	175.520
3	0.9	326.571	1232.713	461.241	1755.204

3. Conclusion

It has been demonstrated that, higher confinement voltages are needed for both QIT and CIT cases when the modulated "index" parameter $k = 0.9$ and the damping force is applied. The ratio of confinement voltage with and without damping force are the same for $k = 0$ and $k = 0.9$. These types of functioning behavior of QIT and CIT, performed different fractional mass resolution as far as theoretical study is concerned. However, it is clear that, at least in the lower mass range the impulse voltage with the damping force is quite suitable for the CIT with higher mass resolution.

References

1 V. I. Baranov, Analytical approach for description of ion motion in quadrupole mass spectrometer, *J. Am. Soc. Mass Spectrom.*, 2003, **14**, 818.
2 V. I. Baranov, Ion energy in quadrupole mass spectrometry, *J. Am. Soc. Mass Spectrom.*, 2004, **15**, 48.
3 E. C. Beaty, Simple electrodes for quadrupole ion traps, *J. Appl. Phys.*, 1987, **61**, 2118.
4 R. Blatt and D. J. Wineland, Entangled states of trapped atomic ions, *Nature*, 2008, **453**, 1008.
5 K. Blaum, High-accuracy mass spectrometry with stored ions, *Phys. Rep.*, 2006, **425**, 1.
6 K. Blaum, F. Herfurth, Trapped Charged Particles and Fundamental Interactions, *Lector Notes in Physics*, Springer, Berlin, 2008, **749**, 99.
7 D. J. Douglas, A. J. Frank and D. M. Mao, Linear ion traps in mass spectrometry, *Mass Spectrom. Rev.*, 2005, **24**, 1.
8 A. P. French, Introduction to Quantum Physics, *Newtonian Mechanics(The M.I.T. Introductory Physics Series)*, (1st ed.). W.W. Norton and Company Inc., New York, 1970, ISBN 393-09958-X.
9 Q. Z. Hu, R. J. Noll, H. Y. Li, A. Makarov, M. Hardman and R. G. Cooks, The Orbitrap: a new mass spectrometer, *J. Mass Spectrom.*, 2005, **40**, 430.
10 W. M. Itano, J. C. Bergquist, R. G. Hulet and D. J. Windeland, Radiative Decay Rates in Hg^+ from Observations of Quantum Jumps in a Single Ion, *Phys. Rev. Lett.*, 1987, **59**, 2732.
11 W. M. Itano, D. J. Heinzen, J. J. Bollinger and D. J. Wineland, Quantum Zeno Effect, *Phys. Rev. A: At., Mol., Opt. Phys.*, 1990, **41**, 2295.
12 D. Kielpinski, V. Meyer, M. A. Rowe, C. A. Sackett, W. M. Itano, C. Monroe and D. J. Wineland, A Decoherence-Free Quantum Memory Using Trapped Ions, *Science*, 2001, **291**, 1013.
13 K. H. Kingdon, A Method for the Neutralization of Electron Space Charge by Positive Ionization at Very Low Gas Pressures, *Phys. Rev.*, 1923, **21**, 408.
14 N. V. Konenkov, M. Sudakov and D. J. Douglas, Matrix methods for the calculation of stability diagrams in quadrupole mass spectrometry, *J. Am. Soc. Mass Spectrom.*, 2002, **13**, 597.
15 O. Kornienko, P. T. A. Reilly, W. B. Whitten and J. M. Ramsey, Electron impact ionization in a microion trap mass spectrometer, *Rev. Sci. Instrum.*, 1999, **70**, 3907.
16 O. Kornienko, P. T. A. Reilly, W. B. Whitten and J. M. Ramsey, Micro ion trap mass spectrometry, *Rapid Commun. Mass Spectrom.*, 1999, **13**, 50.
17 R. E. March, J. F. J. Todd, *Practical Aspects of Ion Trap Mass Spectrometry: Chemical, Environmental, and Biomedical Application*. CRC Press: New York, (1995).
18 R. March, An introduction to quadrupole ion trap mass spectrometry, *J. Mass Spectrom.*, 1997, **32**, 263.
19 R. E. Mather, R. M. Waldren, J. F. J. Todd and R. E. March, Some operational characteristics of a quadrupole ion storage mass spectrometer having cylindrical geometry, *Int. J. Mass Spectrom. Ion Phys.*, 1980, **33**, 201.
20 O. J. Orient and A. Chutjian, A compact, high–resolution Paul ion trap mass spectrometer with electron–impact ionization, *Rev. Sci. Instrum.*, 2002, **73**, 2157.
21 W. Paul and H. Steinwedel, A new mass spectrometer without magnetic field, *Z. Naturforsch*, 1953, **8**(A), 448.
22 R. J. Rafac, B. C. Young, J. A. Beall, W. M. Itano, D. J. Wineland and J. C. Berquist, Sub-dekahertz Ultraviolet Spectroscopy of $^{199}Hg^+$, *Phys. Rev. Lett.*, 2000, **85**, 2462.
23 E. Richard Badman, Miniature cylindrical ion traps and arrays, Purdu University, PhD Thesis, 2001.
24 T. Rosenband, D. B. Hume, P. O. Schmidt, C. W. Chou, A. Brusch, L. Lorini, W. H. Oskay, R. E. Drullinger, T. M. Fortier, J. E. Stalnaker, S. A. Diddams, W. C. Swann, N. R. Newbury, W. M. Itano, D. J. Wineland and J. C. Bergquist, Frequency Ratio of Al^+ and Hg^+ Single–Ion Optical Clocks; Metrology at the 17th Decimal Place, *Science*, 2008, **319**, 1808.
25 S. M. Sadat Kiai, A. R. Zirak, M. Elahi, S. Adlparvar, B. N. Mortazavi, A. Safarien, S. Farhangi, S. Sheibani, S. Alhooie, M. M. A. Khalaj, A. A. Dabirzadeh, M. Ruzbehani and F. Zahedi, Investigation of some structural fusion materials for (n, a) reactions at the 14–15 Mev energy region, *J. Fusion Energy*, 2010, **29**, 412.
26 S. M. Sadat Kiai, J. Andre, Y. Zerega, G. Brincourt and R. Catella, Study of a quadrupole ion trap supplied with a periodic impulsional potential, *Int. J. Mass Spectrom. Ion Processes*, 1991, **107**, 191.
27 S. M. Sadat Kiai, Y. Zerega, G. Brincourt, R. Catella and J. Andre, *Int. J. Mass Spectrom. Ion Processes*, 1991, **108**, 65.

28 S. M. Sadat Kiai, Confinement of ions in a radio frequency quadrupole ion trap supplied with a periodic impulsional potential, *Int. J. Mass Spectrom.*, 1999, **188**, 177.
29 S. M. Sadat Kiai, M. Baradaran, S. Adlparvar, M. M. A. Khalaj, A. Doroudi, S. Nouri, A. A. Shojai, M. Abdollahzadeh, F. D. Abbasi, M. V. Roshan and A. R. BabazadehInt, Impulsional mode operation for a Paul ion trap, *Int. J. Mass Spectrom.*, 2005, **247**, 61–66.
30 S. Seddighi Chaharborj and S. M. Sadat Kiai, Study of a cylindrical ion trap supplied by a periodic impulsional potential, *J. Mass Spectrom.*, 2010, **45**, 111.
31 A. Steane, C. F. Roos, D. Stevens, A. Mundt, D. Leibfried, F. Schmidt-Kaler and R. Blatt, Speed of ion-trap quantum-information processors, *Phys. Rev. A: At., Mol., Opt. Phys.*, 2000, **62**, 1.
32 K. R. Symon, *Mechanics* (Third ed.). Addison-Wesley, 1971, ISBN 0-201-07392-7.
33 J. von Zanther, J. Abel, Th. Becker, M. Fries, E. Peik, H. Walther, R. Holzwarth, J. Reichert, Th. Udem, T. W. Hansch, A. Yu. Nevsky, M. N. Skvortsov and S. N. Bagayev, *Opt. Commun.*, 1999, **166**, 57.
34 D. J. Wineland, W. M. Itano and J. C. Bergquist, Absorption spectroscopy at the limit: detection of a single atom, *Opt. Lett.*, 1987, **12**, 389.
35 X. Wei, S. Qingyu, A. S. Scott, J. C. William and O. Zheng, Ion Trap Mass Analysis at High Pressure: A Theoretical View, *J. Am. Soc. Mass Spectrom.*, 2009, **20**, 2144.
36 J. M. Wells, E. R. Badman and R. G. Cooks, A Quadrupole Ion Trap with Cylindrical Geometry Operated in the Mass-Selective Instability Mode, *Anal. Chem.*, 1998, **70**, 438.
37 B. Whitten William, T. A. Reilly Peter and J. Michael Ramsey, High-pressure ion trap mass spectrometry, *Rapid Commun. Mass Spectrom.*, 2004, **18**, 1749.

